Two-target Lazy Ring: Bimodality, Shortcut Effects, and Exact Mechanism

Model parameters (definitions)

All indices are taken modulo N. The positive direction is defined by increasing node index (clockwise in my sketches).

- N: number of ring nodes.
- n_0: start node.
- (m_1, m_2): absorbing target nodes.
- K: number of ring neighbors per step ($K = 2$ uses ± 1, $K = 4$ uses $\pm 1, \pm 2$).
- q: move probability per step; stay-put probability is $1 - q$.
- g: global drift (bias) parameter; $g > 0$ biases moves in the positive direction.
- β: shortcut strength under the selfloop rule; shortcut probability is $p = \beta(1 - q)$.
- $\mathrm{src}, \mathrm{dst}$: shortcut start and end nodes.
- ρ_k: absorption probability at target m_k (here $\rho_1 = \rho_2 = 1$).

Key findings and figures

I build a **two-target** lazy ring model and provide exact (non-MC) examples of bimodality and trimodality for both **no shortcut** and **selfloop shortcut** settings. Main takeaways:

1. **No shortcut with drift** yields robust bimodality: a fast peak from counter-drift short paths and a slow peak from along-drift long paths (Figs. 2–3).
2. **With shortcut** the distribution decomposes into fast/slow channels; the fast peak is shortcut-dominated while the slow peak is non-shortcut dominated, producing a clear (N, β) bimodal window (Figs. 4–5, 8).
3. **Three-peak example** arises from strong drift plus $K = 4$ jump-over, leading to a layered "per-lap" structure (Fig. 6).

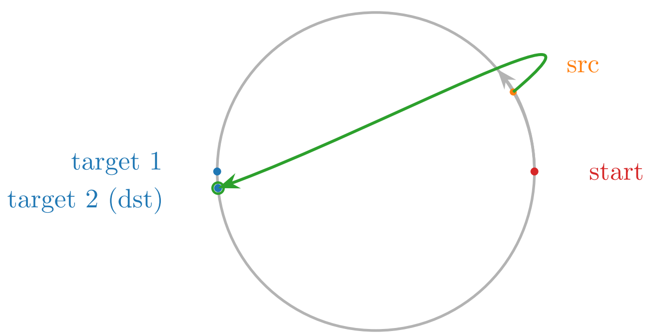

Figure 1: Geometry for the two-target lazy ring with a directed shortcut (parameters of the shortcut cases).

Explicit configurations (all indices modulo N). Start node is always $n_0 = 0$. The two targets and shortcut settings for the representative cases are:

- **Case A (no shortcut, $K = 2$):** $N = 20$, targets $(m_1, m_2) = (18, 10)$, $q = 2/3$, $g = 0.6$, $\beta = 0$.
- **Case B (no shortcut, $K = 4$):** $N = 30$, targets $(m_1, m_2) = (27, 15)$, $q = 2/3$, $g = 0.6$, $\beta = 0$.
- **Cases C/D (shortcut, $K = 2/4$):** $N = 60$, targets $(m_1, m_2) = (30, 31)$, src $= 5$, dst $= 31$, $q = 2/3$, $g = 0$, $\beta = 0.02$.
- **Case E (three-peak, no shortcut, $K = 4$):** $N = 30$, targets $(m_1, m_2) = (29, 20)$, $q = 0.9$, $g = 0.8$, $\beta = 0$.

The same configurations are tabulated in Table 1.

Representative cases: geometry + FPT

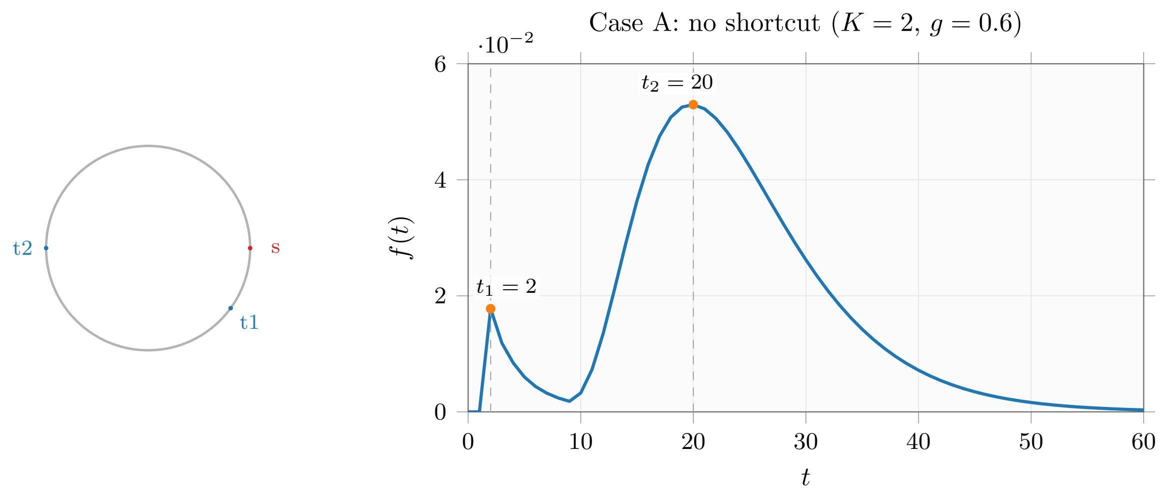

Figure 2: Case A: geometry and bimodal FPT (peaks marked by dots; dashed lines at t_1, t_2).

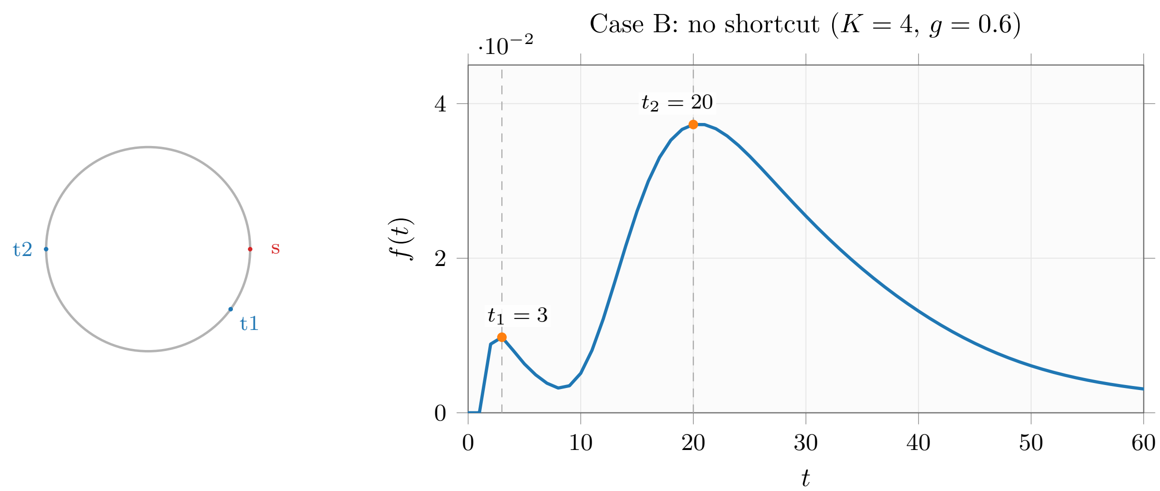

Figure 3: Case B: geometry and bimodal FPT (peaks marked by dots; dashed lines at t_1, t_2).

Model and full two-target absorption mechanism

Lazy ring and drift. The ring has N nodes indexed by $0, 1, \ldots, N-1$. At each step, the walker stays with probability $1 - q$ and moves with probability q. For $K = 2$ (steps ± 1) and

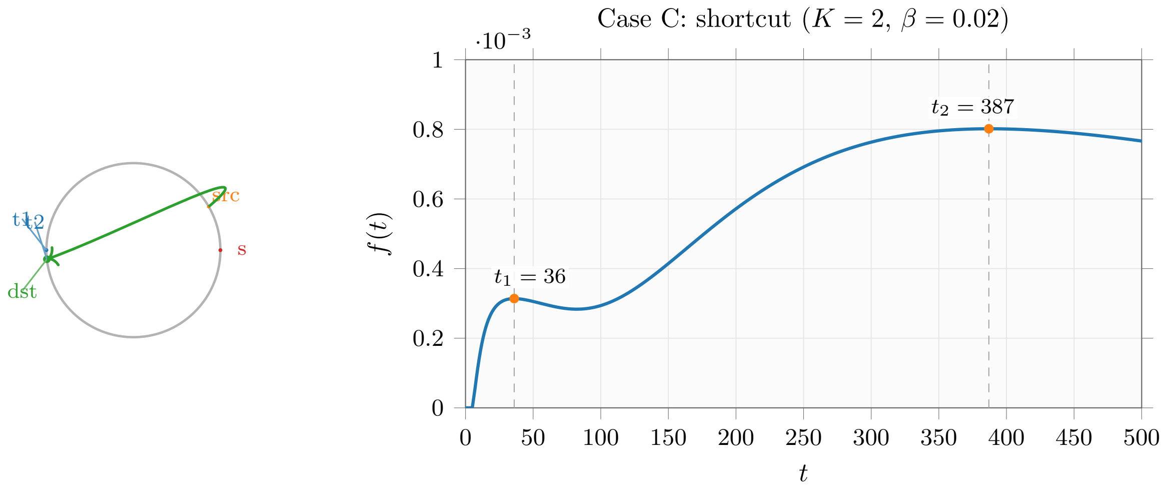

Figure 4: Case C: geometry and bimodal FPT (peaks marked by dots; dashed lines at t_1, t_2).

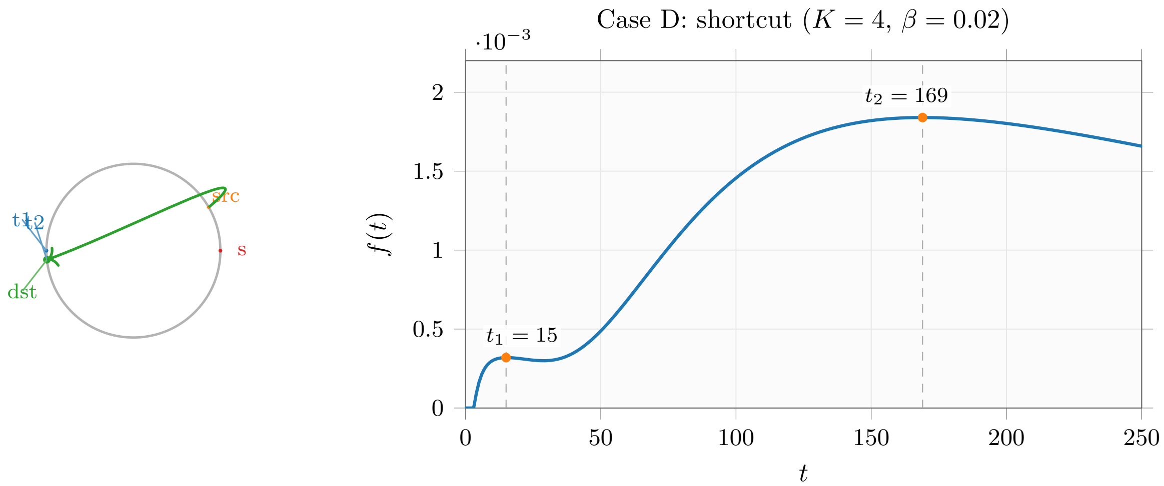

Figure 5: Case D: geometry and bimodal FPT (peaks marked by dots; dashed lines at t_1, t_2).

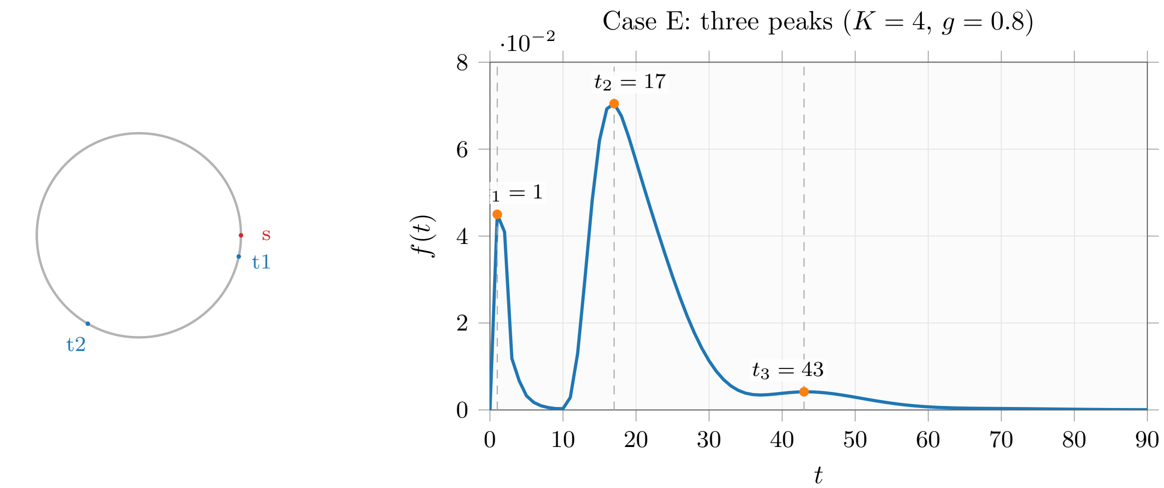

Figure 6: Case E: geometry and three-peak FPT (peaks marked by dots; dashed lines at peak times).

$K = 4$ (steps $\pm 1, \pm 2$), a drift parameter $g \in [-1, 1]$ splits the move probability:

$$P(+) = \frac{q(1+g)}{2}, \qquad P(-) = \frac{q(1-g)}{2}, \tag{1}$$

and the same-direction step lengths share this mass (e.g., for $K = 4$, $+1$ and $+2$ each get $P(+)/2$).

Shortcut (selfloop rule). Only at the source node src, a fraction of the self-loop is diverted to a shortcut src $\to$ dst:

$$p = \beta(1-q), \qquad P(\text{src} \to \text{src}) = 1 - q - p, \qquad P(\text{src} \to \text{dst}) = p. \tag{2}$$

All other nodes follow the base ring dynamics.

Exact two-target recursion. Let m_1, m_2 be absorbing targets. After one step, any mass at the targets is absorbed:

$$\mathbf{p}_{t+1} = \mathbf{p}_t \mathbf{W}, \qquad f_i(t+1) = [\mathbf{p}_{t+1}]_{m_i}, \qquad \mathbf{p}_{t+1}(m_i) = 0,\ i \in \{1, 2\}. \tag{3}$$

Thus $f(t) = f_1(t) + f_2(t)$, and survival is $S(t) = \sum_i p_t(i)$ with $S(t+1) = S(t) - f(t+1)$. This gives the exact time-domain FPT distribution without Monte Carlo.

Absorbing Markov chain form (full mechanism). Partition the transition matrix as

$$\mathbf{W} = \begin{pmatrix} \mathbf{Q} & \mathbf{R} \\ 0 & I \end{pmatrix}, \tag{4}$$

where $\mathbf{Q}$ is the transient subchain and $\mathbf{R}$ contains transitions into the two absorbing states. Let $\mathbf{r}_i$ be the column of $\mathbf{R}$ for target m_i and $\mathbf{p}_0$ be the initial distribution. Then

$$f_i(t+1) = \mathbf{r}_i^{\mathsf{T}} \mathbf{Q}^t \mathbf{p}_0, \qquad f(t+1) = \mathbf{r}^{\mathsf{T}} \mathbf{Q}^t \mathbf{p}_0, \tag{5}$$

with $\mathbf{r} = \mathbf{r}_1 + \mathbf{r}_2$. In generating-function form,

$$\widetilde{f}_i(z) = z\, \mathbf{r}_i^{\mathsf{T}} (I - z\mathbf{Q})^{-1} \mathbf{p}_0. \tag{6}$$

Equivalently, the survival function is

$$S(t) = \mathbf{1}^{\mathsf{T}} \mathbf{Q}^t \mathbf{p}_0, \qquad f(t+1) = S(t) - S(t+1), \tag{7}$$

so the two-target FPT is entirely determined by $\mathbf{Q}$ and the two columns $\mathbf{r}_1, \mathbf{r}_2$. If $\mathbf{Q}$ is diagonalizable, $\mathbf{Q} = \mathbf{V}\boldsymbol{\Lambda}\mathbf{V}^{-1}$, then

$$f(t+1) = \sum_k c_k\, \lambda_k^t, \tag{8}$$

so multiple peaks arise when several modes with distinct time scales (distinct $|\lambda_k|$) carry comparable weights. This is the complete mathematical mechanism: the time-domain distribution is a weighted sum of $\mathbf{Q}$-powers, while the frequency-domain response is governed by the resolvent $(I - z\mathbf{Q})^{-1}$.

Connection to Giuggioli's multi-target formula. For any graph, the single-target first-passage generating function satisfies

$$\widetilde{F}_{i\to j}(z) = \frac{\widetilde{P}_i(j;z)}{\widetilde{P}_j(j;z)}. \tag{9}$$

For two targets, the splitting FPT is a 2×2 determinant ratio[1]. If $G_k = \widetilde{F}_{n_0\to m_k}(z)$ and F_{jk} are built from target-to-target passages and return terms, then

$$\widetilde{F}_{n_0\to(m_1|m_2)}(z) = \frac{G_1F_{22} - F_{12}G_2}{F_{11}F_{22} - F_{12}F_{21}}, \tag{10}$$

with the other target obtained by symmetry. The total FPT is the sum of the two splitting distributions. For partial absorption ρ_k, the diagonal terms become

$$F_{kk} = 1 + \frac{1-\rho_k}{\rho_k}\,[1 - R_{m_k}(z)], \tag{11}$$

where $R_{m_k}(z)$ is the return generating function at target m_k (excluding absorption by the other target). In my $\rho_1 = \rho_2 = 1$ cases, $F_{11} = F_{22} = 1$ and the formula simplifies.

Why multiple peaks appear. Multiple peaks arise from multiple path families / time scales. Drift creates a fast counter-drift family and a slow along-drift family; shortcuts create fast shortcut paths and slow non-shortcut paths. Two targets further split the probability mass and enhance the visibility of separated modes.

No shortcut: drift-driven bimodality

Cases A/B (Figs. 2–3) show drift-driven bimodality without shortcuts; Fig. 7 shows splitting contributions.

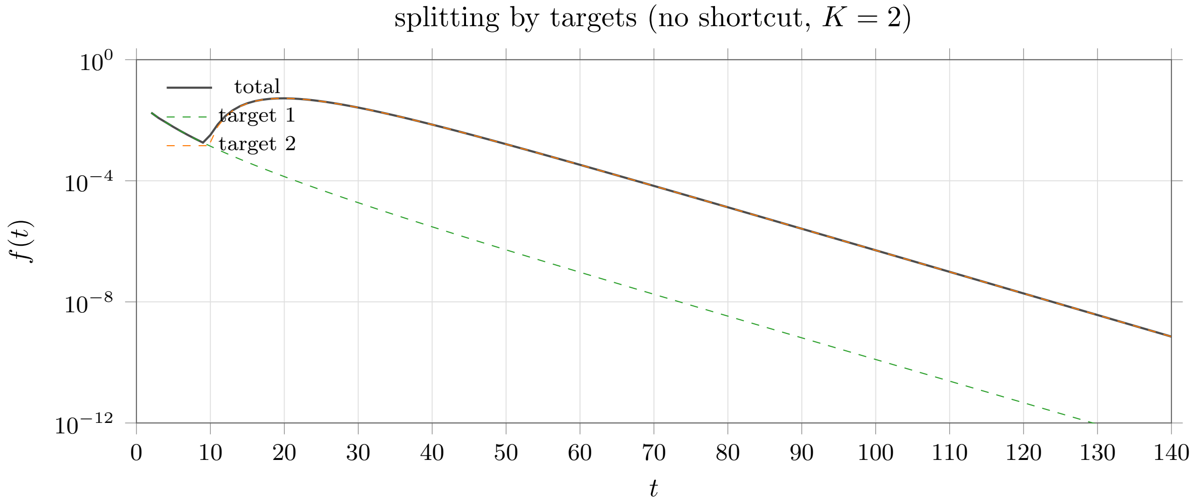

Figure 7: Target splitting: total FPT equals target-1 plus target-2 components.

With shortcut: fast/slow channel superposition

Cases C/D (Figs. 4–5) show shortcut-induced bimodality; Fig. 8 shows the (N,β) bimodality map (0=no, 1=paper, 2=macro).

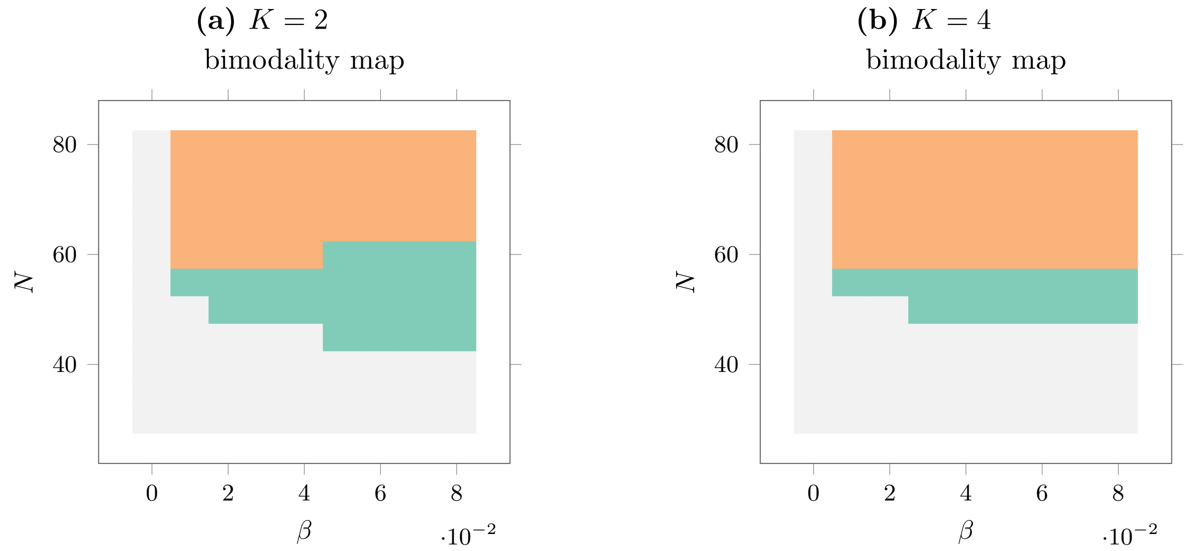

Figure 8: Bimodality map (0=no, 1=paper, 2=macro) with src = 5, dst = m_2, $m_1 = \lfloor N/2 \rfloor$, $m_2 = m_1 + 1$.

Three-peak example

Case E (Fig. 6) shows a three-peak case driven by strong drift and $K = 4$ jump-over.

Configurations and reproducibility

Tables 1 and 2 summarize the representative cases and peak metrics. Reproduce with:

```
cd reports/ring_two_target
python3 code/two_target_report.py
latexmk -pdf -auxdir=build -emulate-aux-dir ring_two_target_en.tex
```

Table 1: Representative configurations (see `data/model_configs.csv`).

Case	N	K	q	g	β	targets
A_no_sc_K2	20	2	0.667	0.60	0.000	(18,10)
B_no_sc_K4	30	4	0.667	0.60	0.000	(27,15)
C_sc_K2	60	2	0.667	0.00	0.020	(30,31)
D_sc_K4	60	4	0.667	0.00	0.020	(30,31)
E_triple_K4	30	4	0.900	0.80	0.000	(29,20)

Table 2: Peak locations and criteria (t_1 earliest peak, t_2 latest peak).

Case	t_1	h_1	t_2	h_2	h_2/h_1	paper	macro
A_no_sc_K2	2	1.78e-02	20	5.30e-02	2.98	True	True
B_no_sc_K4	3	9.78e-03	20	3.73e-02	3.81	True	False
C_sc_K2	36	3.14e-04	387	8.02e-04	2.55	True	True
D_sc_K4	15	3.19e-04	169	1.84e-03	5.76	True	True
E_triple_K4	1	4.50e-02	43	4.17e-03	0.09	True	True

References

[1] L. Giuggioli et al., *Multi-target search in bounded and heterogeneous environments: a lattice random walk perspective*, arXiv:2311.00464v2.

[2] A. Sarvaharman and L. Giuggioli, *Phys. Rev. E* 102, 062124 (2020).